Synthesis and Reactivity of Porphyrinatorhodium(II)−Triethylphosphine Adducts: The Role of PEt_3 in Stabilizing a Formal Rh(II) State

James P. Collman* and Roman Boulatov

Contribution from the Department of Chemistry, Stanford University, Stanford, California 94305

Received April 18, 2000

Abstract: Rh(por)H, where por is an octaethyl- or meso−tetraphenylporphyrin dianion, reacts with triethylphosphine to form stable mononuclear paramagnetic formally-Rh^{II} complexes, Rh(OEP)(PEt_3) and Rh(TPP)(PEt_3)$_2$. The former adduct is also obtained as the sole product of the reaction between $Rh_2(OEP)_2$ and PEt_3. The EPR spectroscopy at 77 K shows both complexes to have mainly porphyrin-based HOMOs. The composition and the reactivity of Rh(TPP)(PEt_3)$_2$ support its formulation as $Rh^{III}(TPP^{\bullet-})(PEt_3)_2$. In contrast, Rh(OEP)($PEt_3$) demonstrates the reactivity of both a Rh^{II} d^7 center and a porphyrin π-anion radical. The adduct reacts with O_2 as a Rh^{II}(por) species, originally forming a Rh^{III}-superoxido derivative. In contrast, with water Rh(OEP)(PEt_3) reacts as a porphyrin π-anion radical, yielding a Rh^{III}−octaethylphlorin complex. The latter is the first characterized phlorin complex of a heavy transition metal. The dual reactivity of Rh(OEP)(PEt_3) is proposed to arise from thermal excitation of the unpaired electron from the porphyrin-based HOMO onto the metal-based LUMO ($d\sigma^*_{Rh-P}$). Unlike the other reported 1:1 adducts of Rh^{II}(por) species with σ-basic ligands, Rh(OEP)(PEt_3) is remarkably stable toward disproportionation to Rh^{I} and Rh^{III}. To understand the origin of this stability, the affinity of $Rh^{III}(OEP)^+$ toward PEt_3 and pyridine was measured spectrophotometrically. The high binding affinity of PEt_3 to Rh(OEP) is proposed as the underlying cause of the increased stability of Rh(OEP)(PEt_3) toward disproportionation.

Introduction

Porphyrin complexes of d^7 metalloradical Rh^{II} demonstrate remarkable reactivity with otherwise rather inert substrates. Activation, under mild conditions, of methane,[1a−c] various benzylic[1b,d] and allylic[1e] C−H bonds, and Si−H and Sn−H bonds[2] have been reported. Facile reactions of Rh^{II}(OEP) (Figure 1) with aliphatic aldehydes and alkynes produce β-formyl complexes[3] and metalloalkenes, (OEP)RhCH═C(R)Rh(OEP),[1e] respectively. Reductive coupling of ethene and acrylates[4,5] as well as alkyl group abstraction from terminal olefins and alkynes,[6] alkyl phosphites,[7a] and alkylisocyanides[7b] by various Rh^{II}(por) species have also been observed. Upon coordination to the Rh^{II}−porphyrin moiety, CO is activated toward a variety of 1-electron carbonyl reactions, such as hydrogen atom abstraction from water,[8a,g] ethanol,[8e,g] primary amines,[7b] and trialkylstannates,[8b] addition to C═C bonds,[8b] and coupling leading to dimetal α-diketones, (por)RhC(O)C(O)Rh(por).[8a−d,f] Rh^{II}(por) complexes react with H_2 and H_2/CO mixtures, yielding metallohydride[1a,9] and metalloformyl[10] derivatives, respectively. Addition of O_2 or NO to Rh^{II}(por) results in quite stable superoxido and nitrosyl complexes, $Rh^{III}(por)(O_2^-)$ and Rh(por)(NO).[11] The former species can undergo further transformations,[11,12] such as conversion to a (μ,η^1,η^1)-peroxo complex.[11]

Despite this remarkable chemistry, applications of Rh^{II}−porphyrin complexes to catalysis are hardly explored. While catalytic activity of both Rh^{III}(por) derivatives[13−15] and Rh^{II} carboxylates[16] in a variety of synthetic organic transformations is well established, Rh^{II}(por) species have only been examined

(1) (a) Zhang, X.-X.; Wayland, B. B. *J. Am. Chem. Soc.* **1994**, *116*, 7897−7898. (b) Wayland, B. B.; Ba, S.; Sherry, A. E. *J. Am. Chem. Soc.* **1991**, *113*, 5305−5311. (c) Sherry, A. E.; Wayland, B. B. *J. Am. Chem. Soc.* **1990**, *112*, 1259−1261. (d) Del Rossi, K. J.; Wayland, B. B. *J. Am. Chem. Soc.* **1985**, *107*, 7941−7944. (e) Ogoshi, H.; Setsune, J.; Yoshida, Z. *J. Am. Chem. Soc.* **1977**, *99*, 3869−3870.

(2) Mizutani, T.; Uesaka, T.; Ogoshi, H. *Organometallics* **1995**, *14*, 4, 341−346.

(3) Del Rossi, K. J.; Zhang, X.-X.; Wayland, B. B. *J. Organomet. Chem.* **1995**, *504*, 47−56.

(4) (a) Paonessa, R. S.; Thomas, N. C.; Halpern, J. *J. Am. Chem. Soc.* **1985**, *107*, 4333−4335. (b) Wayland, B. B.; Poszmik, G.; Fryd, M. *Organometallics* **1992**, *11*, 3534−3542).

(5) (a) Bunn, A. G.; Wayland, B. B. *J. Am. Chem. Soc.* **1992**, *114*, 6917−6919. (b) Wayland, B. B.; Feng, Y.; Ba, S. *Organometallics* **1989**, *8*, 1438−1441.

(6) Anderson, J. E.; Yao, C.-L.; Kadish, K. M. *Organometallics* **1987**, *6*, 706−711.

(7) (a) Wayland, B. B.; Sherry, A. E.; Bunn, A. G. *J. Am. Chem. Soc.* **1993**, *115*, 7675−7684. (b) Poszmik, G.; Carroll, P. J.; Wayland, B. B. *Organometallics* **1993**, *12*, 3410−3417.

(8) (a) Wayland, B. B.; Woods, B. A.; Pierce, R. *J. Am. Chem. Soc.* **1982**, *104*, 302−303. (b) Wayland, B. B.; Sherry, Alan E.; Poszmik, G.; Bunn, A. G. *J. Am. Chem. Soc.* **1992**, *114*, 1673−1681. (c) Sherry, A. E.; Wayland, B. B. *J. Am. Chem. Soc.* **1989**, *111*, 5010−5012. (d) Coffin, V. L.; Brennen, W.; Wayland, B. B. *J. Am. Chem. Soc.* **1988**, *110*, 6063−6069. (e) Zhang, X.-X.; Parks, G. F.; Wayland, B. B. *J. Am. Chem. Soc.* **1997**, *119*, 7938−7944. (f) Wayland, B. B.; Sherry, A. E.; Coffin, V. L. *J. Chem. Soc., Chem. Commun.* **1989**, 662−663. (g) Miller, R. G.; Kyle, J. A.; Coates, G. W.; Anderson, D. J.; Fanwick, P. E. *Organometallics* **1993**, *12*, 1161−6.

(9) (a) Wayland, B. B.; Ba, S.; Sherry, A. E. *Inorg. Chem.* **1992**, *31*, 148−150. (b) Collman, J. P.; Ha, Y.; Guilard, R.; Lopez, M. A. *Inorg. Chem.* **1993**, *32*, 1788−1794.

(10) (a) Farnos, M. D.; Woods, B. A.; Wayland, B. B. *J. Am. Chem. Soc.* **1986**, *108*, 3659−3663. (b) Wayland, B. B.; Van Voorhees, S. L.; Wilker, C. *Inorg. Chem.* **1986**, *25*, 4039−4024. (c) Van Voorhees, S. L.; Wayland, B. B. *Organometallics* **1985**, *4*, 1887−1888.

(11) Wayland, B. B.; Newman, A. R. *Inorg. Chem.* **1981**, *20*, 3093−3097.

(12) (a) Sakurai, H.; Uchikubo, H.; Ishizu, K.; Tajima, K.; Aoyama, Y.; Ogoshi, H. *Inorg. Chem.* **1988**, *27*, 2691−2695. (b) Anderson, J. E.; Yao, C. L.; Kadish, K. M. *Inorg. Chem.* **1986**, *25*, 3224−3228.

10.1021/ja001364u CCC: $19.00
Published on Web 11/14/2000

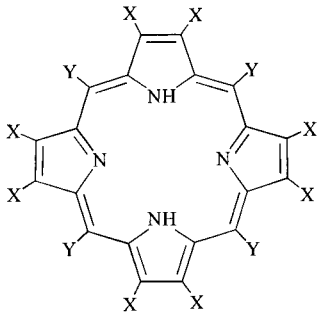

H_2OEP (octaethylporphyrin): X = C_2H_5, Y = H
H_2TPP (meso-tetraphenylporphyrin): X = H, Y = Ph
H_2TTP (meso-tetratolylporphyrin): X = H, Y = p-$C_6H_4CH_3$
H_2TMP (meso-tetramesitylporphyrin): X = H, Y = 2,4,6-$C_6H_2(CH_3)_3$
H_2TTiPP(meso-tetrakis(triisopropylphenyl)porphyrin): X = H, Y = 2,4,6-$C_6H_2{}^iPr_3$

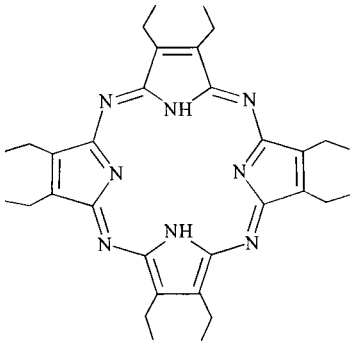

H_2OETAP (octaethyltetraazoporphyrin)

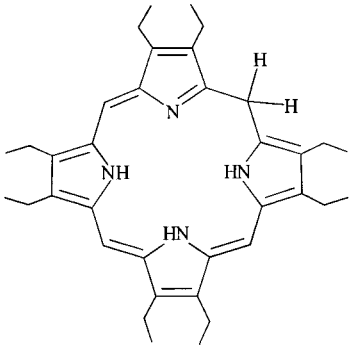

$H_3OEPhlorin$ (octaethylphlorin)

Figure 1. Chemical structures and abbreviations of select porphyrins and octaethylphlorin.

as initiators of free-radical polymerization of acrylates[5b] and photocatalytic production of methanol from CO/H_2 mixtures.[17] Likewise, extensive use of Co^{II}(por) compounds as biomimetic models for respiratory chain enzymes such as cytochrome *c* oxidase,[18a−b] myoglobin, and hemoglobin[18c−d] contrasts sharply with the lack of similar studies involving Rh^{II}(por). This situation persists even though Rh^{II}−porphyrins have a higher affinity toward O_2, and the resulting complexes are more stable, making the relevant intermediates more amenable to characterization.

The paucity of successful work in this area is largely due to the apparent susceptibility of Rh^{II}(por) species to undergo irreversible disproportionation in the presence of simple Lewis bases, such as amines, N-containing heterocycles, and certain phosphines.[7a,19] This makes the design of an appropriate porphyrin-based ligand system that would allow one to take full advantage of the remarkable chemistry of Rh^{II}(por) species much more challenging. While elegant work by Wayland et al.[1a,b,4b,5a,8a] has demonstrated that the porphyrin's peripheral substituents can be used to alter the reactivity of the resulting square-planar Rh^{II}(por) species, an axial ligand L in Rh^{II}(por)L adducts can be expected to have an even more pronounced effect. Prior work by us and others[18d,20] have shown the importance of such axial bases both for directing the substrate binding to a particular face of a metalloporphyrin and for attenuating the reactivity of the trans-bound substrate. While most of this work concerned Fe− and Co−porphyrins, a strong effect of auxiliary ligands on the reactivity of Rh^{II}(por) toward H_2 has also been observed.[9b]

Further progress in this area is not possible without a deeper understanding of the coordination chemistry of the Rh^{II}(por) unit. In the few reports on this subject,[7a,21] two different hypotheses on the mechanism of the ligand-induced disproportionation of Rh^{II}(por) species have been put forward. Wayland et al. proposed that the process is driven by *coordination* of a

(13) Asymmetric cyclopropanation: (a) Bartley, D. W.; Kodadek, T. J. *J. Am. Chem. Soc.* **1993**, *115*, 1656−1660. (b) Brown, K. C.; Kodadek, T. J. *J. Am. Chem. Soc.* **1992**, *114*, 8336−8338. (c) Maxwell, J. L.; Brown, K. C.; Bartley, D. W.; Kodadek, T. J. *Science* **1992**, *256*, 1544−1547. (d) Gross, Z.; Galili, N.; Simkhovich, L. *Tetrahedron Lett.* **1999**, *40*, 1571−1574.

(14) Ketone transformations: (a) Aoyama, Y.; Yamagishi, A.; Tanaka, Y.; Toi, H.; Ogoshi, H. *J. Am. Chem. Soc.* **1987**, *109*, 4735−4737. (b) Aoyama, Y.; Fujisawa, T.; Toi, H.; Ogoshi, H. *J. Am. Chem. Soc.* **1986**, *108*, 943−947.

(15) (a) Asymmetric carbene insertion in the O−H bonds: Hayashi, T.; Kato, T.; Kaneko, T.; Asai, T.; Ogoshi, H. *J. Organomet. Chem.* **1994**, *473*, 323−327. (b) Oxidative carbonylation of amines: Leung, T. W.; Dombek, B. D. *J. Chem. Soc. Chem. Commun.* **1992**, 205−206. (c) Diels−Alder reactions: Bartley, D. W.; Kodadek, T. J. *Tetrahedron Lett.* **1990**, *31*, 6303−6306. (d) Hydroboration−oxidation of olefins: Aoyama, Y.; Tanaka, Y.; Fujisawa, T.; Watanabe, T.; Ogoshi, H. *J. Org. Chem.* **1987**, *52*, 2555−2559.

(16) (a) Padwa, A.; Weingarten, M. D. *J. Org. Chem.* **2000**, *65*, 3722−3732. (b) Doyle, M. P.; Davies, S. B.; Hu, W. *Org. Lett.* **2000**, *2*, 1145−1147. (c) Davies, H. M. L.; Hansen, T.; Churchil, M. R. *J. Am. Chem. Soc.* **2000**, *122*, 3063−3070. (d) Hodgson, D. M.; Stuppie, P. A.; Johnstone, C. *Chem. Commun.* **1999**, 2185−2186. (e) Wood, J. L.; Moniz, G. A.; Pflum, D. A.; Stoltz, B. M.; Holubec, A. A.; Dietrich, H.-J. *J. Am. Chem. Soc.* **1999**, *121*, 1748−1749. (f) Kitagaki, S.; Anada, M.; Kataoka, O.; Matsuno, K.; Umeda, C.; Watanabe, N.; Hashimoto, S. *J. Am. Chem. Soc.* **1999**, *121*, 1417−1418. (g) Davies, H. M. L.; Hansen, T. *J. Am. Chem. Soc.* **1997**, *119*, 9075−9076. (h) Doyle, M. P.; Peterson, C. S.; Parker, D. L. *Angew. Chem., Int. Ed. Engl.* **1996**, *35*, 1334−1336. (i) Davies, H. M. L.; Bruzinski, P.; Hutcheson, D. K.; Kong, N.; Fall, M. J. *J. Am. Chem. Soc.* **1996**, *118*, 6897−6907. (j) Doyle, M. P.; Protopopova, M. N.; Poulter, C. D.; Rogers, D. H. *J. Am. Chem. Soc.* **1995**, *117*, 7281−7282. (k) For reviews, see: Maas, G. *Top. Curr. Chem.* **1987**, *137*, 75−253. Doyle, M. P. *Chem. Rev.* **1986**, *86*, 919−940.

(17) Bosch, H. W.; Wayland, B. B. *J. Chem. Soc., Chem. Commun.* **1986**, 900−901.

(18) (a) Yu, H.-Z.; Baskin, J. S.; Steiger, B.; Anson, F. C.; Zewail, A. H. *J. Am. Chem. Soc.* **1999**, *121*, 484−485. (b) Anson, F. C.; Shi, C.; Steiger, B. *Acc. Chem. Res.* **1997**, *30*, 437−444. (c) Steiger, B.; Baskin, J. S.; Anson, F. C.; Zewail, A. H. *Angew. Chem., Int. Ed.* **2000**, *39*, 257−259. (d) Collman, J. P.; Fu, L. *Acc. Chem. Res.* **1999**, *32*, 455−463.

(19) DeWit, D. G. *Coord. Chem. Rev.* **1996**, *147*, 209−246.

(20) Mamenteau, M.; Reed, C. *Chem. Rev.* **1994**, *94*, 659−698.

(21) (a) Grass, V.; Lexa, D.; Momenteau, M.; Saveant, J.-M. *J. Am. Chem. Soc.* **1997**, *119*, 3536−3542. (b) Ni, Y.; Fitzgerald, J. P.; Carroll, P.; Wayland, B. B. *Inorg. Chem.* **1994**, *33*, 2029−2035. (c) Wayland, B. B.; Balkus, K. J.; Farnos, M. D. *Organometallics* **1989**, *8*, 950−955. (d) Kadish, K. M.; Hu, Y.; Boschi, T.; Tagliatesta, P. *Inorg. Chem.* **1993**, *32*, 2996−3002. (e) Kadish, K. M.; Araullo, C.; Yao, C.-L. *Organometallics* **1988**, *7*, 1583−1587.

donor molecule to one of the disproportionation products, Rh^{III}(por).[7a] In contrast, Saveant et al. more recently suggested[21a] that disproportionation is due to the *deligation* of the original $Rh^{II}(por)L_x$ adduct. Moreover, they and others[21d,e] have also shown that electrochemical reduction of $Rh^{III}(TPP)P_2^+$ adducts ($P = PEt_3$, PMe_2Ph) yields species that were stable on the time scale of their experiments, in a striking contrast with redox behavior of other Rh^{III}−porphyrin derivatives. This result was interpreted as an indication that these phosphines stabilize the Rh^{II} state toward disproportionation.[21a]

In the current paper, we describe the synthesis and reactivity of Rh(OEP)(PEt_3) and Rh(TPP)(PEt_3)$_2$ complexes, which result from addition of PEt_3 to the corresponding metallohydrides, Rh(por)H, as well as reaction of $Rh_2(OEP)_2$ with PEt_3. The particular choice of the porphyrins was determined by their very different electronic properties and sterically compact nature. This, in conjunction with the previous work on sterically encumbered Rh(TMP)(PEt_3),[7a] (Figure 1) provides an opportunity to probe the effects of both electronic and steric factors on distribution of unpaired electron density in, and hence reactivity of, Rh^{II}(por) adducts with PEt_3.

Results

Rh(por)H. The Rh−H bond in porphyrinatorhodium(III) hydrides undergoes facile homolysis such that in solution Rh(por)H exists in equilibrium with Rh^{II}(por) (or the corresponding dimer) and H_2.[10b,22] Coordination of NO to Rh(OEP)H was reported to facilitate the decomposition of the hydride.[11] We anticipated seeing a similar effect in the case of PEt_3.[23] Indeed, addition of PEt_3 to Rh(por)H yields a paramagnetic species as expected from a monomeric Rh^{II} complex. However, Rh(por)H obtained via the traditional aqueous route yielded products that were too unstable to be isolated. To increase the stability of the target adducts, we have examined alternative syntheses of the metallohydride. A reaction between thoroughly dried Rh(por)I and $LiAlH_4$ under rigorously anhydrous conditions yielded Rh(por)H suitable for further synthetic transformations.

Remarkably, Rh(TPP)H obtained under such anhydrous conditions exhibits properties quite different from those appearing in the literature. For example, Rh(TPP)H and Rh(TTP)H were reported[10b] to show significant broadening of ^{1}H NMR resonances ascribed to extensive homolysis of the Rh−H bond. The hydride signals could not be observed unless the solutions were pressurized with H_2 (0.4−1 atm). In contrast, anhydrous Rh(TPP)H demonstrates very sharp resonances, even under vacuum (Figure 2), and H_2 has no effect on their position or shape. Moreover, the Rh−H bond is retained even if a sample of Rh(TPP)H is pyrolyzed for 72 h at 230 °C under vacuum (5 μTorr) or heated at reflux in a toluene solution under strictly anaerobic and anhydrous conditions.

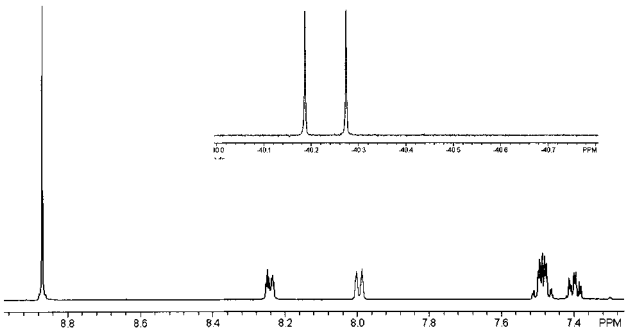

Figure 2. ^{1}H NMR spectrum of HRh(TPP) in C_6D_6 in an evacuated NMR tube.

Rh(TPP)(PEt_3)$_2$ and Rh(OEP)(PEt_3). Addition of PEt_3 to a benzene solution of Rh(OEP)H results in rapid formation of an intermediate adduct, (PEt_3)Rh(OEP)H. The hydride resonance in its ^{1}H NMR spectrum appears as a broad singlet (fwhh = 220 Hz) at −26.5 ppm. The broadening of the signal is too large for the fine structure from the ^{31}P−^{1}H and ^{103}Rh−^{1}H spin couplings to be resolved. However, the 13.8 ppm downfield shift of the hydride resonance in Rh(OEP)(PEt_3)H relative to its position in Rh(OEP)H (−40.8 ppm) is consistent with the coordination of a strongly basic ligand trans to the hydride. Smaller downfield shifts are observed in similar adducts with weaker donors, such as pyridine[21c] and methyl isocyanide[8d] (−32.95 ppm in pyRh(OEP)H and −27.9 ppm in (MeNC)Rh(OEP)H). Unlike these adducts, (PEt_3)Rh(OEP)H can be isolated, but it undergoes hydrogen elimination over a period of several hours. The resulting Rh(OEP)(PEt_3) demonstrates broadened paramagnetically shifted NMR resonances, whose position is dependent on the presence of excess PEt_3 in the sample.

On the other hand, no intermediate adducts were detected in the reaction between the phosphine and Rh(TPP)H. Addition of subequivalent amounts of PEt_3 in a sealed NMR tube results in a decrease in intensity, but no change in position of the Rh(TPP)H resonances, indicating that formation of Rh(TPP)(PEt_3)$_2$ is strongly favored. Under the conditions of excess PEt_3, no broadening of the phosphine's resonances is observed by ^{1}H NMR, suggesting that if exchange between the coordinated and free ligand occurs, it is slow on the NMR time scale.

Similarly, $Rh_2(OEP)_2$ reacts rapidly with an excess of PEt_3 in toluene to give Rh(OEP)(PEt_3) without detectable intermediates or disproportionation products.

The anisotropic EPR signals of both adducts are rather similar (Figure 3). The relatively small g values (Table 1), although not unusual for Rh^{II} complexes, are much closer to those observed for porphyrin π-anion radicals than for the d_{z^2}-based radicals, Rh^{II}(TMP) and Rh^{II}(TPP). The modest ^{31}P-superhyperfine (shf) coupling also suggests that, under the conditions of the EPR experiments, the unpaired electron is located on a mainly porphyrin-based orbital in both Rh(OEP)(PEt_3) and Rh(TPP)(PEt_3)$_2$. Apparently, formation of the Rh−P bond causes such destabilization of the resulting metal-based $d\sigma^*_{Rh-P}$ (d_{z^2}) orbital that its energy becomes higher than that of the LUMO of the porphyrin ligand ($p\pi^*_{por}$). According to calculations, another strong σ-base, H^-, causes similar destabilization of the Rh-based $d\sigma^*_{Rh-H}$ orbital relative to the porphyrin-based $p\pi^*_{por}$.[27] In contrast, observation of a Rh-based EPR signal in Rh(TMP)(PEt_3) indicates that destabilization of $d\sigma^*_{Rh-P}$ in

(22) Setsune, J.; Yoshida, Z.; Ogoshi, H. *J. Chem. Soc., Perkin Trans. 1* **1982**, 983−987.

(23) It is conceivable that coordination of PEt_3 may promote heterolytic cleavage of the Rh−H bond, resulting in transferring H^- to an appropriate organic substrate, such as the porphyrin macrocycle itself. In this case, formation of a diamagnetic Rh^{III}−phlorin complex is expected. Our results suggest that this does not occur to an appreciable extent. Small amounts of Rh^{III}−phlorin complex, along with Rh(OEP)(PEt_3)$_2^+$, are detected in the reaction mixtures. However, addition of PEt_3 to a solution of $Rh_2(OEP)_2$ also produces traces of the phlorin, even though the dimer is incapable of transferring a H^-. The result is likely due to the disproportionation of OEP radical anion (vide infra) in the presence of traces of adventitious water. However, the phosphine-promoted hydride transfer from Rh(por)H may occur in the presence of an appropriate substrate. Indeed, Saveant observed hydride transfer from electrochemically generated $[Rh^{II}(por)H]^-$ to DMSO, as well as electrocatalytic evolution of H_2 from HRh(por) in the presence of a mineral acid and PEt_3, presumably occurring by hydride transfer: Grass, V.; Lexa, D.; Saveant, J.-M. *J. Am. Chem. Soc.* **1997**, *119*, 7526−7532.

(24) Seth, J.; Bocian, D. F. *J. Am. Chem. Soc.* **1994**, *116*, 143−153.

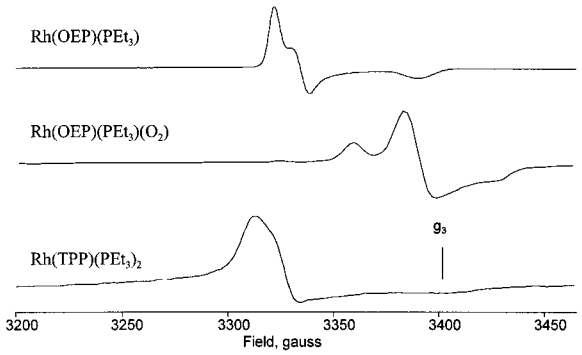

Figure 3. EPR spectra of Rh(OEP)(PEt_3), Rh(OEP)(PEt_3)(O_2), and Rh(TPP)(PEt_3)$_2$ in toluene glass at 77 K; υ = 9.4000 GHz.

Table 1. EPR Parameters for Rh(OEP)(PEt_3), (O_2)Rh(OEP)(PEt_3), and Rh(TPP)(PEt_3)$_2$ and Some Relevant Literature Data

complex	g_1, g_2 (A[^{31}P], MHz)	g_3 (A[^{31}P], MHz)	ref
Rh(OEP)(PEt_3)	2.018 (22.2)	1.982	*a*
Rh(TPP)(PEt_3)$_2$	2.021	1.973	*a*
$H_2OEP^{\bullet-}$	2.0030	2.0021	24
$H_2TPP^{\bullet-}$	2.0029	2.0020	24
Zn($OEP^{\bullet-}$)	2.0027	1.989	24
Rh(TPP)	2.46	∼2	25
Rh(TMP)	2.65	1.915	8c
Rh(TMP)(PEt_3)	2.116 (948)	2.004 (1154)	7a
Rh(OETAP)py$_2$	1.998 (g_{iso})		21b
Rh(OEP)(PEt_3) (O_2)	2.002, 1.982	1.964	*a*
Rh(OEP)(O_2)	2.100	1.988	11
Rh(OEP)(P[OBu]$_3$)(O_2)	2.084 (63), 2.004 (61)	2.000 (66.3)	11
Rh^{II}(5,5′-thiosalicylic acid)	1.962	1.952	26a
Rh^{II}(cysteinato-*O*-methyl)$_2$	2.003 (g_{iso})		26b

[a] Present work.

this complex is insufficient to raise it above pπ^*_{TMP}, even though the latter orbitals are lower in energy than the corresponding pπ^*_{OEP} orbitals in Rh(OEP)(PEt_3). This suggests that the overlap between the d_{z^2} orbital of Rh and the donor orbitals of the PEt_3 ligand is less efficient in Rh(TMP)(PEt_3), probably due to the increased Rh−P separation resulting from unfavorable steric interactions between the peripheral substituents of TMP and the phosphine.

Both EPR and ^{1}H NMR spectra of the OEP adduct support the 1:1 phosphine-to-metal ratio. The composition of the TPP analogue cannot be determined unambiguously by either spectroscopy. This question of stoichiometry was thus addressed by oxidizing these reactive, paramagnetic adducts into stable, diamagnetic derivatives with 1 equiv of an outer-sphere oxidizing agent, $FeCp_2^+$. The resulting species demonstrate ^{1}H NMR and mass spectral properties that are identical to those of authentic samples of Rh(OEP)(PEt_3)$^+$ and Rh(TPP)(PEt_3)$_2^+$ complexes (see Experimental Section). The composition of Rh(OEP)(PEt_3) determined via this method is in agreement with its EPR and ^{1}H NMR spectra. This strongly suggests that the composition of Rh(TPP)(PEt_3)$_2^+$ also correctly reflects a Rh:2P stoichiometry of the initial paramagnetic Rh(TPP)−phosphine adduct.

The UV−visible spectra of Rh(OEP)(PEt_3) (as 100−10 μM toluene solutions) are complicated (Figure 4). Deconvolution

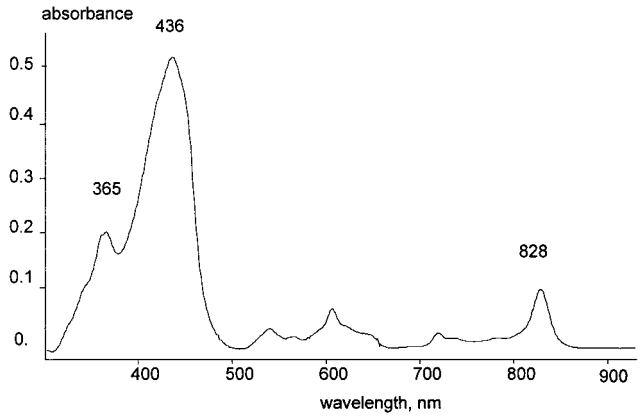

Figure 4. UV−visible spectrum of Rh(OEP)(PEt_3) in toluene/3 M PEt_3.

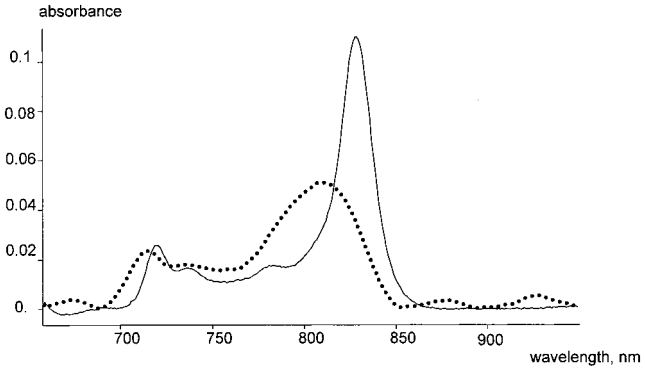

Figure 5. Comparison of the low-energy parts of UV−visible spectra of Rh(OEP)(PEt_3) (solid line) and Rh(OEPhlorin)(PEt_3)$_2$ (dotted line) in toluene/3 M PEt_3.

of the high-energy band centered at 436 yields at least four Gaussian peaks at 401, 420, 436, and 454 nm, presumably belonging to four different Rh(por) derivatives. The complexity of the 500−700-nm region also suggests the presence of several absorbing species. The low-energy part of the spectrum is noteworthy: both porphyrin anion radicals and phlorins are known to possess adsorption bands over 700 nm. However, the differences in the UV−visible spectra of Rh(OEP)(PEt_3) and an authentic sample of a Rh(phlorin) complex (Figure 5) suggest that the low-energy transitions in the spectrum of the former more likely belong to an OEP-anion radical derivative.[28]

The probable multicomponent composition of UV−visible samples of Rh(OEP)(PEt_3) contrasts sharply with the purity of its bulk samples assessed by the EPR and NMR spectroscopies and via oxidation with $FeCp_2^+$. The differences are likely due to *partial* dissociation of the adduct, and a variety of subsequent chemical reactions taking place under the conditions of the relatively low concentration of the analyte in the UV−visible samples. Indeed, concentrated toluene solutions of Rh(OEP)(PEt_3) change color from bright green to red-brown upon dilution. The comparatively small extinction coefficients of porphyrin anion radical derivatives ensure that even relatively small fractions of porphyrin-based decomposition impurity would have a profound effect on the observed UV−visible spectra.

Reactivity of Rh(TPP)(PEt_3)$_2$ and Rh(OEP)(PEt_3). Rh(TPP)(PEt_3)$_2$ demonstrates rather limited reactivity. The complex

(25) Hoshino, M.; Yasufuki, K.; Konishi, S.; Imamura, M. *Inorg. Chem.* **1984**, *23*, 1982−1984.
(26) (a) Srivastava, P. C.; Pandeya, K. B.; Nigam, H. L. *Ind. J. Chem.* **1975**, *13*, 85−86. (b) Pneumatikakis, G.; Psaroulis, P. *Inorg. Chim. Acta* **1980**, *46*, 97−98.
(27) Irie, R.; Li, X.; Saito, Y. *J. Mol. Catal.* **1984**, *23*, 23−27.
(28) We are aware of only one other reported UV−visible spectrum of an OEP anion radial derivative: the spectrum of Ni($OEP^{\bullet-}$) was claimed to have the lowest energy transition at 623 nm;[29] this seems inconsistent with the presence of near-IR absorption bands in anion radicals of deuteroporphyrin and mesoporphyrin IX[30] and TPP[31] derivatives; the absorption bands in the 700−900-nm region are also expected in the OEP anion radical derivatives.[32]

is very oxygen-sensitive, converting into $Rh^{III}(TPP)(PEt_3)_2^+$ within hours even in the solid state in a drybox, presumably by reaction with adventitious O_2. No other products have been detected (by either EPR or ^1H NMR) upon deliberate addition of O_2 to $Rh(TPP)(PEt_3)_2$. Since the superoxido complex, $(TPP)Rh(O_2)$, is stable enough to withstand chromatography,[11] it is unlikely to be an undetected intermediate in the oxidation of $Rh(TPP)(PEt_3)_2$. We believe that a reaction between the $TPP^{\bullet-}$ anion radical and O_2 is more probable. The further fate of the formed superoxide anion, $O_2^{\bullet-}$, is not entirely clear, since a ^1H NMR spectrum of the resulting $Rh(TPP)(PEt_3)_2^+$ did not show peaks attributable to a possible anion, whose nature is at present unknown.

In contrast, $Rh(OEP)(PEt_3)$ reacts with O_2 at −77 °C to form a paramagnetic superoxido complex, $Rh^{III}(OEP)(PEt_3)_x(O_2^{\bullet-})$ ($x = 0, 1$) (Figure 3, Table 1). At higher temperatures, the species rapidly converts to a diamagnetic derivative, as evidenced by disappearance of the EPR signal. We assign the final product as a (μ,η^1,η^1)-peroxo dimer, $(PEt_3)(OEP)Rh{-}OO{-}Rh(OEP)(PEt_3)$, on the basis of its ^1H NMR spectrum and the literature data.[11]

Whether the superoxido complex contains a coordinated phosphine molecule could not be determined definitively. The absence of ^{31}P shf coupling in its EPR spectrum is not conclusive since only a small degree of mixing between the mainly oxygen-based LUMO and the phosphine orbitals is expected. Indeed, very modest ^{31}P shf coupling constants are observed in $Rh(por)(P[OBu]_3)(O_2)$ (Table 1). However, we saw rapid disappearance of the EPR signal, consistent with the presence of an auxiliary ligand, but not with an unligated 5-coordinated $Rh(OEP)(O_2)$, which is known to be rather slow to convert to the μ-peroxo derivative.[11] Likewise, both the known high affinity of PPh_3 to $Rh(TPP)(O_2)$[12b] and the presence of the phosphine ligand in the μ-peroxo dimer suggest that the reaction between $Rh(OEP)(PEt_3)$ and O_2 likely yields the 6-coordinate phosphine adduct $Rh(OEP)(PEt_3)(O_2)$, even though its EPR spectrum does not reveal the spin coupling to the phosphorus atom.

Addition of water to $Rh(OEP)(PEt_3)$ produces a Rh^{III}−phlorin complex (Figure 1). The resulting reaction mixture is rather complex due to the presence of variously ligated Rh^{III} species, but $Rh^{III}(OEP)(PEt_3)_2^+$ and $Rh^{III}(OEPhlorin)(PEt_3)_2$ can be isolated upon addition of an excess of PEt_3. The literature NMR data on phlorin derivatives are very limited,[29] but certain features of the ^1H NMR spectrum of the latter complex, such as loss of the ring current and the 4-fold symmetry of the porphyrin core, clearly indicate a metallophlorin. For example, meso-hydrogens and the methylene groups of the peripheral ethyl substituents of the macrocycle experience an *upfield* shift, relative to their positions in $Rh^{III}(OEP)(PEt_3)_2^+$, of about 4 and 1.5 ppm, respectively. Concomitantly, the phosphine group resonances shift *downfield* by about 5 (CH_2) and <3 ppm (CH_3). This reversed order of the phosphine signals indicates that the chemical shifts of the hydrogen atoms on axial ligands in a metallophlorin−phosphine adduct are no longer determined by the through-space interaction with the ring current.

Stability Constants of $Rh^{III}(OEP)L_x^+$ ($L = PEt_3$, py; $x = 1, 2$) Adducts. The reason for measuring the affinities of these two ligands to the $Rh^{III}(OEP)$ moiety was 2-fold. A reaction between $Rh_2(OETAP)_2$ and pyridine yields the bispyridine adduct, $Rh^{III}(OETAP^{\bullet-})py_2$.[21b] In contrast, only a monoligated complex, $Rh(OEP)(PEt_3)$, can be isolated from solutions of $Rh_2(OEP)_2$ even in neat PEt_3. Therefore, the first goal was to understand whether the difference in the number of the axial ligands in these two adducts is due to a lower intrinsic affinity of the $Rh^{III}(por)$ moiety for PEt_3 than pyridine. Second, the high stability of $Rh(OEP)(PEt_3)$ toward disproportionation contrasts with the rapid decomposition of the analogous Rh^{II} complex, Rh(OEP)py.[21c] The two existing hypotheses on the mechanism of disproportionation of $Rh^{II}(por)L$ adducts propose that the affinity of Rh to the axial ligand, L, determines, albeit in opposite ways, susceptibility of these adducts to disproportionation. Knowledge of both the relative affinities of pyridine and PEt_3 to the $Rh^{III}(OEP)$ moiety, and the relative stabilities of their adducts with $Rh^{II}(OEP)$ toward disproportionation, makes it possible to evaluate the plausibility of each hypothesis.

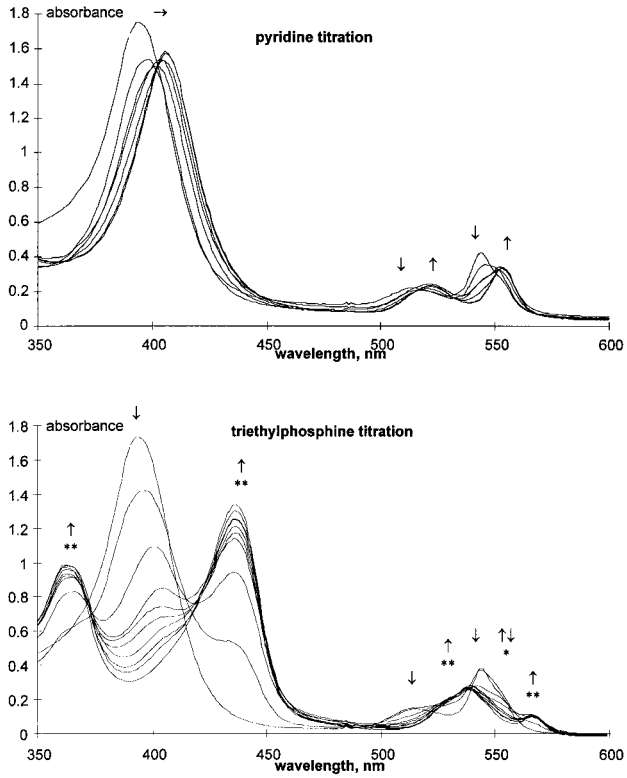

Figure 6. Spectrophotometric titration of 10^{-5} M solutions of $Rh(OEP)(PF_6)$ in toluene with PEt_3 and pyridine. For clarity, only every other UV−visible trace is shown. Single and double asterisks indicate signals corresponding to $Rh(OEP)(PEt_3)PF_6$ and $Rh(OEP)(PEt_3)_2PF_6$, respectively.

To eliminate competition by the counterion or solvent for the metal coordination sites, we carried out spectrophotometric titrations on $Rh(OEP)PF_6$ in toluene under anhydrous and anaerobic conditions (Figure 6). The unligated $Rh^{III}(OEP)^+$ complex was reported[33] to exist as a dimer, $Rh_2(OEP)_2^{2+}$, in relatively concentrated CH_2Cl_2 solutions. The most characteristic feature of the UV−visible spectrum of the dimer is a low-intensity adsorption around 800 nm and split blue-shifted Soret band. The monomer, on the other hand, is expected to have a

(29) Stolzenberg, A. M.; Stershic, M. T. *J. Am. Chem. Soc.* **1988**, *110*, 6391−6402.

(30) Peychal-Heiling, G.; Wilson, G. S. *Anal. Chem.* **1971**, *43*, 545−556.

(31) (a) Lanese, J. G.; Wilson, G. S. *J. Electrochem. Soc.* **1972**, *119*, 1039−1043. (b) Closs, G. L.; Closs, L. E. *J. Am. Chem. Soc.* **1963**, *85*, 818−819. (c) Kadish, K. M. *Prog. Inorg. Chem.* **1986**, *34*, 435−605 and references therein. (d) Grodkowski, J.; Neta, P.; Hambright, P. *J. Phys. Chem.* **1995**, *99*, 6019−6023. (e) Sutter, T. P. G.; Rahimi, R.; Hambright, P.; Bommer, J. C.; Kumar, M.; Neta, P. *J. Chem. Soc., Faraday Trans.* **1993**, *89*, 495−502.

(32) Fuhrhop, J.-H.; Kadish, K. M.; Davis, D. G. *J. Am. Chem. Soc.* **1973**, *95*, 5140−5147.

(33) Lee, S.; Mediati, M.; Wayland, B. *J. Chem. Soc., Chem. Commun.* **1994**, 2299−2300.

Table 2. Stability Constant of Porphyrinatorhodium(III) Adducts and Related Compounds

starting complex	axial ligand	solvent	log K_1	Log K_2	ref
$Rh(OEP)^+$	PEt_3	toluene	6.7± 0.4	4.4 ± 0.4	a
$Rh(OEP)^+$	pyridine	toluene	4.5 ±0.4	< 2	a
$Rh(TPP)^+$	PPh_3	THF[b]	not measd	3.1	21d
(Me)Rh(TPP)	PPh_3	CH_2Cl_2	3.6		21e
(Me)Rh(OEP)	PPh_3	CH_2Cl_2	3.3		21e
(O_2)Rh(TPP)	PPh_3	CH_2Cl_2	5.52		12b
$Rh_2(O_2CCH_3)_4$	$P(CH_2CH_2CN)_3$	AcN[b]	6.26	4.86	34
$Rh_2[O_2CCH_2(OMe)]_4$	pyridine	H_2O[b]	4.52 ± 0.02	2.81 ± 0.04	35

[a] Present work. [b] Solvent occupies free coordination sites.

single Soret peak centered around 400 nm. A saturated solution of $Rh(OEP)^+$ in toluene (~30 μM) demonstrates both sets of signals; however, dilution to 10 μM concentration effectively eliminates the peaks corresponding to the dimer. Attempts to mathematically process a set of titration data performed on a saturated toluene solution of $Rh(OEP)^+$ were unsuccessful. Therefore, studies were done on 10 μM solutions to minimize complications associated with the presence of equilibria involving the dimer and possibly its derivatives.

The titration results (Table 2) show that PEt_3 forms more stable adducts with Rh^{III}(por) than pyridine does. The rather large ratio of the subsequent stability constants ($K_1/K_2 = 230$ for PEt_3) probably reflects the mutual destabilization of the two quite basic ligands trans to each other. A similarly higher affinity of phosphine relative to pyridine for Rh^{II} centers in μ-carboxylate dimers has been reported. The smaller K_1/K_2 ratio found in these bimetallic carboxylate systems is consistent with a decrease in electronic interactions between the two axial ligands upon separation by the Rh−Rh bond. The stability constants of other Rh(por)−phosphine adducts reported in the literature are slightly smaller than those for $Rh(OEP)(PEt_3)_2^+$, which can probably be attributed mostly to the noncoordinating, nonpolar properties of toluene used in our measurements. Such a medium destabilizes the higher charge density species and does not compete for the free coordination sites.

Discussion

Nature of the HOMO in Rh(por)$(PEt_3)_x$ Adducts. Paramagnetic complexes $Rh(OEP)(PEt_3)$ and $Rh(TPP)(PEt_3)_2$ were obtained upon addition of PEt_3 to the corresponding metallohydrides, Rh(por)H. The chemistry of these adducts and their potential as catalysts are determined by whether the unpaired electron is located on the metal or on the macrocycle. The HOMO of square-planar Rh^{II}(por) complexes is d_{z^2}, but upon formation of an adduct, Rh(por)L, this orbital acquires antibonding character with respect to the Rh−L bond. The ensuing destabilization may lead to a reversal of ordering, whereupon the porphyrin-based $p\pi^*_{por}$ orbitals become the HOMO and the metal-based $d\sigma^*_{Rh-L}$ becomes the LUMO of the adduct. The high symmetry of the adducts nearly eliminates mixing between the $p\pi^*_{por}$ and $d\sigma^*_{Rh-L}$ (d_{z^2}) orbitals. Therefore, such adducts can normally be characterized as *either* Rh^{II}(por) derivatives (the HOMO is $d\sigma^*_{Rh-L}$), *or* Rh^{III} complexes of porphyrin anion radical, $Rh^{III}(por^{\bullet-})L_x$ (the HOMO is $p\pi^*_{por}$), with the correspondingly different chemistry and composition.

To the first class belong several monoadducts of Rh^{II}(TMP) and Rh^{II}(TTiPP) (Figure 1) with amines, pyridines, and phosphines trapped at low temperature.[7a] They demonstrate a metal-based EPR signal, do not form bis-adducts even in the presence of an excess of a ligand, and rapidly disproportionate at temperatures above 77 K. Due to such instability, their reactivity beyond susceptibility to disproportionation is unexplored. The second type of adduct is exemplified by a bispyridine species,

Scheme 1. Summary of the Reactivity of $Rh(OEP)(PEt_3)$ and $Rh(TPP)(PEt_3)_2$

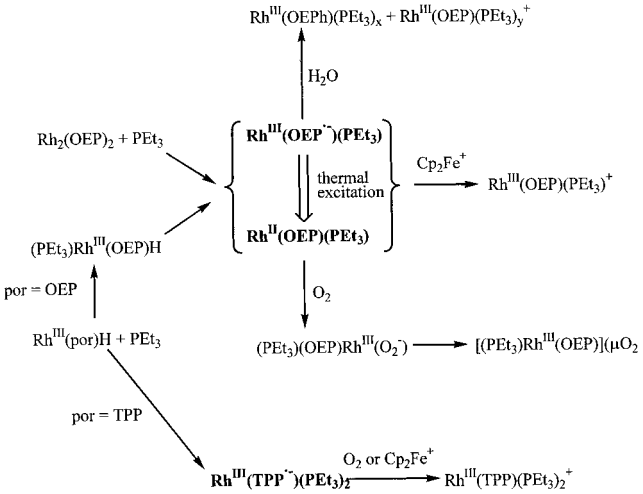

$Rh(OETAP)py_2$, which is formed in a pyridine solution of a Rh^{II} complex, $Rh_2(OETAP)_2$.[21b] Its EPR and UV−visible spectra are consistent with a porphyrin anion radical, and the compound is stable toward disproportionation. Similar adducts, Rh(TPP)P_2 (P = PEt_3, PMe_2Ph) were obtained by one-electron reduction of the corresponding Rh^{III} bisphosphine complexes.[21a,d,e] Although the species were not isolated, UV−visible spectroscopy showed them to be Rh^{III}-porphyrin anion radical derivatives. The adducts did not disproportionate on the time scale of a spectroelectrochemical measurement.[36]

In this work, we prepared and isolated $Rh(TPP)(PEt_3)_2$ in quantities sufficient to study its physicochemical properties more thoroughly, and they are consistent with the adduct being a Rh^{III}−porphyrin anion radical complex. Its EPR spectrum demonstrates relatively small values of g and ^{31}P shf indicative of a porphyrin-based radical. Bis-adducts are not known in the chemistry of Rh^{II}(por) species, since such 19-electron species should be susceptible to facile loss of the second axial ligand. In contrast, $Rh(TPP)(PEt_3)_2$ is very stable toward dissociation, as evidenced by ^1H NMR experiments and the fact that the complex does not produce any detectable amount of a superoxido complex upon exposure to O_2 (Scheme 1). A 5-coordinate dissociation product, $Rh(TPP)(PEt_3)$, is expected to form an adduct with dioxygen.

The situation with $Rh(OEP)(PEt_3)$ is more complex. Its low-temperature EPR spectrum is similar to that of $Rh(TPP)(PEt_3)_2$

(34) Macartney, D. H., Aquino, M. A. S. *Inorg. Chem.* **1987**, *26*, 2696−2699.

(35) Das, K.; Simmons, E. L.; Bear, J. L. *Inorg. Chem.* **1977**, *16*, 1268−1278.

(36) $Rh(TPP)(PEt_3)_2$ was formulated as a Rh^{II} complex;[21a] this is obviously a misinterpretation of the UV−visible spectrum, which closely resembles those of $H_2TPP^{\bullet-}$ and $Zn(TPP^{\bullet-})$[31] but is very different from a spectrum of a genuine porphyrinatorhodium(II) complex, Rh^{II}(TMP).[37]

indicating that the HOMO of the adduct is mainly porphyrin-based $p\pi^*_{por}$. At room temperature, Rh(OEP)(PEt_3) reacts with H_2O as a porphyrin anion radical, producing a phlorin derivative (Scheme 1).[29,30] On the other hand, its reaction with O_2 yields a superoxido complex, (PEt_3)Rh(OEP)(O_2), which suggests that the unpaired electron is located on the metal-based orbital.[38] Likewise, our failure to isolate the bisphosphine complex, Rh(OEP)(PEt_3)$_2$, even from solutions of Rh(OEP)(PEt_3) in neat phosphine is consistent with the dissociation lability of 19-electron 6-coordinate Rh^{II} species, but contradicts the high affinity of Rh^{III}(OEP) to PEt_3, and the fact that other $Rh^{III}(por^{\bullet-})$ complexes are obtained only as bisligated species. Thus, depending on experimental conditions, Rh(OEP)(PEt_3) appears to react as either Rh^{II}(OEP)(PEt_3) or $Rh^{III}(OEP^{\bullet-})(PEt_3)$. A plausible explanation of these observations is that the nearly mutually orthogonal orbitals, $p\pi^*_{por}$ and $d\sigma^*_{Rh-P}$ are close in energy so that at 200−300 K the unpaired electron is thermally promoted from the lower-lying $p\pi^*_{por}$ to $d\sigma^*_{Rh-P}$. At 77 K, the population of the higher energy $d\sigma^*_{Rh-P}$ is apparently insufficient to generate a detectable Rh-based radical signal by EPR. At higher temperatures, the excited state becomes sufficiently populated to determine the reactivity of Rh(OEP)(PEt_3) with certain substrates (such as O_2 and PEt_3, but not H_2O).

Thus, the much richer chemistry of Rh(OEP)(PEt_3) as compared to similar complexes Rh(OETAP)py_2 and Rh(TPP)-(PEt_3)$_2$ apparently arises from the higher energy of the lowest-lying acceptor orbitals of OEP relative to OETAP or TPP. This decreases the energy gap between the porphyrin-based HOMO ($p\pi^*_{OEP}$) and the metal-based LUMO ($d\sigma^*_{Rh-P}$) in the OEP complex to such an extent that the $(p\pi^*_{OEP})^0(d\sigma^*_{Rh-P})^1$excited state appears to become important in determining the reactivity of Rh(OEP)(PEt_3).

Susceptibility of Rh(por)L toward Disproportionation. For ligands, such as pyridine or alkylphosphines, that have comparable affinity to both Rh^{III} and Rh^{II}, disproportionation of corresponding 1:1 adducts, Rh(por)L, to $Rh^{III}(por)L_2^+$ and $Rh^{I}(por)^-$ (reaction 1) is probably always thermodynamically favorable irrespective of the exact location of the unpaired electron (that is whether the HOMO of Rh(por)L is metal-based or porphyrin-based). On the other hand, π-acidic ligands, such as CO, which have much lower affinity to Rh^{III} than Rh^{II}, should stabilize the +2 state and thus suppress disproportionation. The situation is more complex for 1:2 adducts, Rh(por)L_2 (reaction 2), since the loss of the Rh−L bonds may not be compensated by the higher stability of Rh(por)L_2^+ and Rh(por)$^-$. Indeed, some bis-adducts (Rh(TPP)(PEt_3)$_2$, Rh(OETAP)py_2)[21b] are stable, while others (pyRh(TMP)Cl)[31d] disproportionate rapidly. Likewise, the monoligated Rh^{II}(por) species with σ-donors, such as Rh(TMP)(PEt_3)[7a] and Rh(OEP)py,[1c] undergo facile disproportionation, while the corresponding 1:1 CO adducts, Rh(por)-CO, are stable.[7a,8b] Rh(OEP)(PEt_3) is unique in being a stable 1:1 adduct of Rh(por) with a simple σ-donor ligand.

$$2\mathrm{Rh(por)L} \rightarrow \mathrm{Rh(por)L_2}^+ + \mathrm{Rh^I(por)}^- \qquad (1)$$

$$2\mathrm{Rh(por)L_2} \rightarrow \mathrm{Rh(por)L_2}^+ + \mathrm{Rh^I(por)}^- + 2\mathrm{L} \qquad (2)$$

The mechanism of the disproportionation is not yet well established, with two conflicting hypotheses proposed to date (Scheme 2). According to mechanism A,[21a] disproportionation requires partial dissociation of the adduct, yielding the nonligated Rh^{II}(por), whose reducing properties relative to those of Rh(por)L are enhanced due to the square-planar 4-coordinate environment favored by Rh^{I}. This mechanism is similar to that proposed for disproportionation of $Rh^{II}(bipy)_3^{2+}$.[39] Thus, Rh^{II}(por)L adducts that have high dissociation stability are predicted to be less susceptible to disproportionation. An alternative hypothesis[7a] (mechanism B) proposes that disproportionation is driven by association step 3b (Scheme 2) and consequently leads to the opposite conclusion. Higher affinity ligands make formation of the Rh^{III} complex, $Rh^{III}(por)L_2^+$, more favorable, and therefore, the corresponding adducts should be more susceptible to disproportionation.

Scheme 2. Two Possible Mechanisms for Disproportionation of Rh^{II}(por)L Adducts[a]

(1a) $(por)Rh^{II}L \rightleftharpoons (por)Rh^{II} + L$

(2a) $(por)Rh^{II}L + (por)Rh^{II} \longrightarrow (por)Rh^{III}L^+ + [(por)Rh^{I}]^-$

Mechanism A

(1b) $(por)Rh^{II}L + (por)Rh^{II}L \rightleftharpoons (por)Rh^{III}L^+ + (por)Rh^{I}L^-$

(2b) $(por)Rh^{I}L^- \longrightarrow [(por)Rh^{I}]^- + L$

(3b) $(por)Rh^{III}L^+ + L \longrightarrow (por)Rh^{III}L_2^+$

Mechanism B

[a] The superscripts refer to the formal oxidation state of Rh and do not imply the actual distribution of the unpaired electron density.

In the present work, we have shown that PEt_3 has a higher affinity to $Rh^{III}(por)^+$ than pyridine; similar results have been obtained by others[34,35] for Rh^{II} complexes (Table 2). We have also shown that Rh(OEP)(PEt_3) is stable toward disproportionation, while a similar adduct with pyridine, Rh(OEP)py, is known to decompose rapidly to $Rh^{III}(OEP)py_2^+$ and $Rh^{I}(OEP)^-$.[21c] These data, in our opinion, suggest that among simple σ-donor ligands, those with higher affinity for Rh^{III}, impart higher stability to their adducts, Rh(por)L. The higher disproportionation susceptibility of Rh(TMP)(PEt_3) relative to Rh(OEP)(PEt_3) is consistent with the presumed lower dissociation stability of the former adduct, due to the unfavorable steric interactions between the peripheral substituents of the porphyrin and PEt_3. Such a weaker Rh−P bond in Rh(TMP)(PEt_3) versus Rh(OEP)-(PEt_3) is suggested by the EPR spectra of these adducts.

Reaction between $Rh_2(OEP)_2$ and PEt_3. There are several synthetic advantages in using metallohydrides Rh(por)H, as opposed to the corresponding dimers, $Rh_2(por)_2$, as precursors to Rh(por)L adducts. First, the dimer is usually obtained from the hydride (or the related derivatives), and the direct conversion of Rh(por)H into Rh(por)L shortens the synthesis. Second, such dimerization is normally done under relatively harsh or difficult to control conditions, which makes it less suitable for elaborate porphyrin derivatives. However, there are important reasons to study the interactions between $Rh_2(por)_2$ and donor molecules.

The Rh^{II} dimers in non-porphyrin environments show a high propensity to add one or two ligands trans to the Rh−Rh bond. Considerable theoretical[40] and experimental[41] efforts have been directed toward elucidating details of such adduct formation. Similar reactivity of the Rh_2^{4+} core in the porphyrin environment has been much less studied. The well documented decomposition

(37) Vitols, S. E.; Friesen, D. A.; Williams, D. S.; Melamed, D.; Spiro, T. G. *J. Phys. Chem.* **1996**, *100*, 207−213.

(38) An alternative mechanism would be an oxidation of the porphyrin anion radical by O_2, forming $Rh^{III}(por)^+$ and $O_2^{\bullet-}$, followed by a rapid collapse of the resulting ion pair; as far as we are aware, such a mechanism of formation of superoxido complexes has never been demonstrated; a direct reaction between a Rh^{II} center and O_2 seems more plausible.

(39) (a) Brown, G. M.; Chan, S. F.; Creutz, C.; Schwartz, H. A.; Sutin, N. *J. Am. Chem. Soc.* **1979**, *101*, 7638−7640. (b) Mulazzani, Q. G.; Emmi, Hoffman, M. Z.; Venturi, M. *J. Am. Chem. Soc.* **1981**, *103*, 3362−3370. (c) For other examples of Rh^{II} disproportionation thought to proceed via redox exchange between differently ligated species, see: Haefner, S. C.; Dunbar, K. R.; Bender, C. *J. Am. Chem. Soc.* **1991**, *113*, 9540−9553.

of $Rh_2(por)_2$ in the presence of donor molecules[7,21c,42] is often driven by irreversible processes such as alkyl group abstraction, or disproportionation of monomeric Rh^{II}(por)L adducts, and does not necessarily reflect the reactivity of the dimer. Among the very few reported systems where such side reactions do not occur, only CO and related arylisocyanides form bimetallic adducts, $(CO)Rh_2(OEP)_2$[8d] and $(ArNC)Rh_2(OEP)_2$,[7b] while $Rh_2(OETAP)_2$ undergoes homolytic Rh−Rh bond cleavage in the presence of pyridine.[21b] We have now shown that another σ-donor, PEt_3, causes homolysis of the Rh−Rh bond in $Rh_2(OEP)_2$. These limited data suggest that the Rh−Rh bond cleavage is promoted by the auxiliary ligands that interact particularly strongly with the $d\sigma_{Rh-Rh}$ orbital (PEt_3)[40d,e] or by the porphyrins that have particularly low-lying acceptor orbitals (OETAP). This is equivalent to saying that ligand-induced dissociation of $Rh_2(por)_2$ appears to occur when the interaction between the donor orbitals of the axial ligand(s) and the $d\sigma_{Rh-Rh}$ orbital is sufficient to raise the latter's energy above that of the porphyrin's LUMO. The resulting adduct dissociates because it has zero Rh−Rh bond order: $d\pi^4\delta^2(\delta^*)^2(d\pi^*)^4(p\pi^*_{por})^2(d\sigma)^0$. It is well known that axial ligation of non-porphyrin Rh^{II} dimers induces such destabilization of the $d\sigma_{Rh-Rh}$ orbital that in many cases it becomes the HOMO of the resulting adduct.[40e,43]

An interesting implication of this hypothesis is that certain auxiliary ligands may enhance the metalloradical reactivity of sterically unencumbered Rh^{II}(por) complexes. Such species are less active than their sterically bulky analogues,[1b] since their facile dimerization decreases the amount of the reactive d^7 monomer, Rh^{II}(por). An appropriate porphyrin−auxiliary ligand combination would induce just sufficient destabilization of the $d\sigma_{Rh-Rh}$ orbital to cause dissociation of $Rh_2(por)_2$, but to retain the Rh^{II}(por) reactivity of the resulting 5-coordinate adducts. Rh(OEP)(PEt_3) exemplifies this concept.

Conclusions

Paramagnetic complexes, Rh(OEP)(PEt_3) and Rh(TPP)-(PEt_3)$_2$, result from addition of PEt_3 to the corresponding metallohydrides, Rh(por)H, under rigorously anaerobic and anhydrous conditions. According to low-temperature EPR studies, the HOMO of both complexes is mainly porphyrin-based, not the metal-based $d\sigma^*_{Rh-P}$ (d_{z^2}) as is the case in related Rh(TMP)(PEt_3).[7a] The difference is probably due to less efficient overlap of d_{z^2} and donor orbital of the phosphine in the TMP adduct, expected to result from the unfavorable steric interactions between the peripheral substituents of TMP and PEt_3.

The composition and reactivity of the TPP derivative support that it is a Rh^{III} complex of TPP anion radical, $Rh^{III}(TPP^{\bullet-})(PEt_3)_2$, similar to the previously reported Rh(OETAP)py_2.[21b] This conclusion is also in agreement with the spectroelectrochemically obtained UV−visible spectrum of Rh(TPP)(PEt_3).[21a] In contrast, Rh(OEP)(PEt_3), demonstrates the reactivity of both Rh^{II}(OEP) and $Rh^{III}(OEP^{\bullet-})$ species, depending on the substrate. It reacts with H_2O forming a phlorin derivative, according to the known reactivity of porphyrin anion radicals.[29,30,31d,e] However, its reaction with O_2, yielding a Rh^{III}−superoxido complex, is identical to that of Rh^{II} species, such as $Rh_2(OEP)_2$.[11] We propose that this dual reactivity is due to thermal promotion of the unpaired electron from porphyrin-based HOMO onto the metal-based $d\sigma^*_{Rh-P}$ LUMO.

Unlike analogous 1:1 adducts, Rh(TMP)(PEt_3) and Rh(OEP)-py, Rh(OEP)(PEt_3) is not susceptible to disproportionation. This difference, along with the data on relative affinities of pyridine and PEt_3 to $Rh^{III}(por)^+$, supports the previously proposed hypothesis that disproportionation of such adducts is determined by their dissociation stability.

Experimental Section

General Information. All synthetic manipulations were done in a Vacuum Atmosphere's drybox ([O_2] < 1 ppm) or on a vacuum line, using standard procedures and Schlenk glassware. Solvents were degassed and distilled off sodium (toluene and PEt_3), sodium benzophenone ketyl (benzene, pentane, pyridine), or P_2O_5 (CH_2Cl_2, $CDCl_3$) under Ar prior to use. $FeCp_2PF_6$ was recrystallized twice from anhydrous acetonitrile/toluene under rigorously anaerobic conditions, dried under vacuum (5 mTorr), and stored in a drybox; $AgPF_6$ was dried at 40 °C for 12 h under vacuum and stored in a drybox. H_2OEP,[44] H_2TPP,[45] $Rh_2(CO)_4Cl_2$,[46] and $Rh_2(OEP)_2(PF_6)_2$[33] were synthesized according to published procedures. ^1H NMR spectra were taken on a Varian's UnityInova 500-MHz spectrometer and are reported in ppm vs TMS. UV−visible and EPR spectra were taken on Hewlett-Packard 8453 and Brucker ER 220D-SRC spectrometers, respectively. All ^1H NMR and UV−visible spectra were taken at 25.0 ± 0.1 °C. Mass spectrometry was performed at the Mass Spectrometry Facility, University of California at San Francisco.

Rh(por)I. This synthesis follows a modified published procedure:[47] under N_2, H_2por (100 mg) and $Rh_2(CO)_4Cl_2$ (100 mg, 0.22 mmol) are dissolved in anhydrous CH_2Cl_2 (10 mL), anhydrous NaOAc (500 mg, 6 mmol) is added, and a stream of N_2 is adjusted such that the solvent evaporates within 45 min. Avoiding exposure to air, the reaction mixture is dried further under dynamic vacuum (5 min, to remove residual acetic acid), a new portion of CH_2Cl_2 (10 mL) is added, and the procedure is repeated. The reaction mixture is dissolved in dry benzene (10 mL), and I_2 (1.1 equiv) is added at once. The progress of oxidation is monitored by UV−visible and TLC, and as soon as the reaction is complete (10 min for H_2OEP and 45 min for H_2TPP), the mixture is transferred to a silica column; the product is eluted with CH_2Cl_2, and dried under dynamic vacuum (50 μTorr) at 100 °C for 24 h. Yields: 85−90% for IRh(OEP), 75−80% for IRh(TPP); some $[Rh(CO)_2]_2$TPP is recovered and can be reused. Longer reaction times

(40) (a) Eagle, C. T.; Farrar, D. G.; Pfaff, C. U.; Davies, J. A.; Kluwe, C.; Miller, L. *Organometallics*, **1998**, *17*, 4523−4526. (b) Kawamura, T.; Maeda, M.; Miyamoto, M.; Usami, H.; Imaeda, K.; Ebihara, M. *J. Am. Chem. Soc.* **1998**, *120*, 8136−8142. (c) Cotton, F. A.; Feng, X. *J. Am. Chem. Soc.* **1998**, *120*, 3387−3397. (d) Sargent, A. L.; Rollog, M. E.; Eagle, C. T. *Theor. Chem. Acc.* **1997**, *97*, 283−288. (e) For a comprehensive review of older literature, see: Boyar, E. B.; Robinson, S. D. *Coord. Chem. Rev.* **1983**, *50*, 109−208.

(41) (a) Cotton, F. A.; Dikarev, E. V.; Petrukhina, M. A.; Stiriba, S.-E. *Inorg. Chem.* **2000**, *39*, 1748−1754. (b) Cotton, F. A.; Dikarev, E. V.; Petrukhina, M. A.; Stiriba, S.-E. *Organometallics* **2000**, *19*, 1402−1405. (c) Cotton, F. A.; Dikarev, E. V.; Petrukhina, M. A. *J. Organomet. Chem.* **2000**, *596*, 130−135. (d) Pruchnik, F. P.; Starosta, R. Liz, T.; Lahuerta, P. *J. Organomet. Chem.* **1998**, *568*, 177−183. (e) Crawford, C. A.; Matonic, J. H.; Huffman, J. C.; Folting, K.; Dunbar, K. R.; Christou, G. *Inorg. Chem.* **1997**, *36*, 2361−2371. (f) Pirrung, M. C.; Morehead, A. T. *J. Am. Chem. Soc.* **1994**, *116*, 8991−9000. (g) Nicolo, F.; Bruno, G.; Lo Schiavo, S.; Sinicropi, M. S.; Piraino, P. *Inorg. Chim. Acta* **1994**, *223*, 145−149. (h) For a comprehensive review of older literature, see: Felthouse, T. R. *Prog. Inorg. Chem.* **1982**, *29*, 73−165.

(42) (a) Feng, M.; Chan, K. S. *J. Organomet. Chem.* **1999**, *584*, 235−239. (b) Wayland, B. B.; Woods, B. A. *J. Chem. Soc., Chem. Commun.* **1981**, 475−476.

(43) Structurally related Rh^{II}phthalocyanine dimer, $Rh_2(pc)_2$, forms a very stable 1:2 adduct with pyridine, $py_2Rh_2(pc)_2$ (Huckstadt, H.; Bruhn, C.; Homborg, H. *J. Porphyrins Phthalocyanines* **1997**, *1*, 367−378). The dimer manifests a Rh−Rh distance (2.741(2) Å) comparable to that in other trans L−Rh−Rh−L units, containing an unsupported Rh−Rh bond, and significantly shorter than the Rh−Rh bond length in $(PPh_3)_2Rh_2(dmg)_4$ (dmg = dimethylglyoxime monoanion, 2.936(2) Å).[41h] This suggests that unfavorable van der Waals interactions between porphyrin cores in putative $LRh_2(por)_2$ and $L_2Rh_2(por)_2$ adducts are probably not the main reason for their instability.

(44) Sessler, J. L.; Mozaffari, A.; Johnson, M. R. *Org. Synth.* **1992**, *70*, 68−78.

(45) Adler, A. D.; Longo, F. R.; Finarelli, J. D.; Goldmacher, J.; Assour, J.; Korsakoff, L. *J. Org. Chem.* **1967**, *32*, 476.

(46) McCleverty, J. A.; Wilkinson, G. *Inorg. Synth.* **1990**, *28*, 84−86.

(47) Abeysekera, A. M.; Grigg, R.; Trocha-Grimshaw, J.; Viswanatha, V. *J. Chem. Soc., Perkin Trans. 1* **1977**, 1395−1403.

or excess of I_2 in our hands did not increase the degree of conversion of $[Rh(CO)_2]_2TPP$: IRh(OEP) ^1H NMR ($CDCl_3$) δ 10.31 (s, 4H, meso), 4.23 (m, 6.5 Hz, 8H, CH_2), 4.10 (m, 6.5 Hz, 8H, CH_2), 2.00 (t, 6.5 Hz, 24H, CH_3); UV−vis (toluene, λ_{max}/nm); 352, 402, 518, 551. IRh(TPP) ^1H NMR ($CDCl_3$) δ 8.96 (s, 8H, β-pyrolic), 8.27 (d, 6 Hz, 4H, o-Ph), 8.02 (d, 6 Hz, 4H, o′-Ph), 7.50 (m, 8H, m, m′-Ph), 7.38 (m, 4H, p-Ph); UV−vis (toluene, λ_{max}/nm) 422, 533, 565.

Rh(por)H. In a drybox, rigorously dried Rh(por)I (100 mg) is dissolved in anhydrous benzene (50 mL) and $LiAlH_4$ (5.5 mg, 1.1 equiv) is added. The mixture is stirred for 20 h at room temperature in the dark, after which the progress of the reaction is monitored by UV−visible and ^1H NMR spectroscopies every hour. Once the conversion is complete, the precipitates have to be filtered quickly in order to avoid accumulation of an unidentified impurity. The filtrate yields Rh(por)H in a quantitative yield after removal of C_6H_6 in vacuo: HRh(OEP) ^1H NMR (C_6D_6) δ 10.15 (s, 4H, meso), 3.94 (q, 8.5 Hz, 16H, CH_2), 1.88 (t, 8.5 Hz, 24H, CH_3), −40.30 (d, $^1J(^{103}Rh,H) = 45$ Hz); UV−vis (toluene, λ_{max}/nm) 394, 509, 544, 600. HRh(TPP) ^1H NMR (C_6D_6) δ 8.87 (s, 8H, β-pyrolic), 8.24 (dt, 8.5 Hz, 2.5 Hz, 4H, o-Ph), 7.99 (d, 8.5 Hz, 4H, o′-Ph), 7.49 (m, 8H, m-,m′-Ph), 7.40 (tm, 8 Hz, 8H, p-Ph), −40.23 (d, $^1J(^{103}Rh,H) = 44$ Hz); UV−vis (toluene, λ_{max}/nm) 415, 521, 580, 605.

$Rh_2(OEP)_2$. HRh(OEP) (5 mg) was heated at 200 °C under dynamic vacuum (5 μTorr) overnight in a pyrolytic tube. HRh(OEP) partially sublimes but can be returned to the heated part of the tube. Conversion is quantitative after two cycles: ^1H NMR (C_6D_6) δ 9.28 (s, 4H, meso), 4.43 (m, 7 Hz, 8H, CH_2), 3.95 (m, 7 Hz, 8H, CH_2), 1.71 (t, 8 Hz, 24H, CH_3); UV−vis (toluene, λ_{max}/nm) 384, 427, 450, 488, 518, 543, 636.

Rh(OEP)(PEt_3). In a drybox, HRh(OEP) (20 mg; 30 μmol) is suspended in anhydrous toluene (5 mL) and PEt_3 (5 mL of a 3 M solution in toluene; 0.13 mmol, 4 equiv) is added. In one method, the mixture is allowed to stir at room temperature overnight. The color changes from red to brown within 2 h. ^1H NMR spectrum of the reaction mixture indicates formation of (PEt_3)Rh(OEP)H (21−20 (very br s, 16H), 10.3 (br s), −0.7 (br s, 24H), −1.3 (very br s), −2.4 (very br s), −26.5 (s, hydride)). The reaction mixture becomes bright green after ∼8 h. Toluene and the phosphine are removed under reduced pressure and the product is extracted with toluene (The red residue contains $Rh(OEP)(PEt_3)_2^+$; ^1H NMR spectroscopy does not reveal signals attributable to the anion, but it is likely hydroxide. This side product could result from reactions of Rh(OEP)(PEt_3) with traces of adventitious O_2 (followed by ligand displacement) and/or H_2O. The latter reaction also yields the small detected amount of the phlorin complex—vide infra). The toluene is removed to give a green precipitate of Rh(OEP)-(PEt_3), which is washed with pentane (3 mL) to remove a small amount of the phlorin side product, $(PEt_3)_2$Rh(octaethylphlorin). Yield: 60−65%. Alternatively, a toluene solution of the starting materials is placed in a J. Young flask (50 mL), the headspace evacuated, and the mixture heated in an oil bath at 80−85 °C for 2 h, followed by a regular workup. (CAUTION: Heating a liquid in a sealed container presents a potential explosion hazard; adequate precautions should be taken!). The yields are ∼50% but the resulting Rh(OEP)(PEt_3) is somewhat more stable to decomposition. Rh(OEP)(PEt_3) can also be prepared from $Rh_2(OEP)_2$ by dissolving it in a 1.5 M solution of PEt_3 in toluene; the solution becomes green immediately, and removal of toluene/PEt_3 yields a green powder with properties identical to that of Rh(OEP)(PEt_3) prepared from HRh(OEP): ^1H NMR (C_6D_6) δ 21 (very br, 15H, phosphine), 10.2 (br, 16H, CH_2), −0.7 (br, 24H, CH_3); UV−vis (3 M PEt_3/toluene, λ_{max}/nm) 361, 420 (sh), 436, 451(sh), 540, 564, 606, 620, 647, 721, 740, 784, 828 (See the Results section).

Reactivity of Rh(OEP)(PEt_3). (1) Rh(OEP)(PEt_3)(O_2). A 100−μL sample of a 2 mM solution of Rh(OEP)(PEt_3) is placed in an EPR tube fitted with a J. Young valve, the solution is frozen with liquid N_2, the headspace is evacuated, the solution is warmed to −77 °C, the tube is refilled with dry air (the color becomes to change from green to red), the content is mixed rapidly, and the solution is frozen with liquid N_2.

(2) $[Rh(OEP)(PEt_3)]_2(\mu O_2)$. The EPR sample is allowed to warm within 5 min; the resulting compound is stable in air at room temperature: ^1H NMR (C_6D_6) δ 10.4 (br, 4H, meso), 4.1 (br, 16H, CH_2), 1.9 (br, 24H, CH_3), −1.9 (br, 9H, phosphine CH_3), −3.4 (br, 6H, phosphine CH_2); UV−vis (toluene, λ_{max}/nm) 422, 530, 560, 606. An identical complex is formed if a toluene solution of Rh(OEP)(PEt_3) is allowed to stir for several days in a drybox.

(3) $(PEt_3)_2$Rh(octaethylphlorin). A 10-mL sample of degassed water-saturated toluene is added to 1 mL of a 10 mM solution of Rh(OEP)(PEt_3) in toluene; the color changes to red. The resulting reaction mixture has a very complex ^1H NMR spectrum, due to the presence of differently ligated species. To simplify the interpretation of the results, an excess of PEt_3 is added, the reaction mixture is allowed to stir for 10 min, solvents are removed under reduced pressure, and $(PEt_3)_2$Rh(octaethylphlorin) is extracted in pentane: ^1H NMR (C_6D_6) δ 6.31 (s, 2H, meso), 5.62 (s, 2H, meso), 5.42 (s, 1H, meso), 2.72 (q, 7.5 Hz, 4H, CH_2), 2.54 (q, 7.5 Hz, 4H, CH_2), 2.51 (q, 7.5 Hz, 4H, CH_2), 2.50 (q, 7.5 Hz, 4H, CH_2), 1.62 (qt, 8 Hz, 2.5 Hz ($^{31}P-H$), 12 H, phosphine CH_2), 1.27 (t, 7.5 Hz, 6H, CH_3), 1.24 (t, 7.5 Hz, 6H, CH_3), 1.22 (t, 7.5 Hz, 6H, CH_3), 1.20 (t, 7.5 Hz, 6H, CH_3), 0.68 (t, 8 Hz, 18 H, phosphine CH_3); UV−vis (3 M PEt_3/toluene, λ_{max}/nm): 332, 434, 540, 568, 606, 714, 811 (br).

(4) Oxidation with $FeCp_2PF_6$. An aliquot of a stock solution of $FeCp_2PF_6$ (0.045 mmol) in CH_2Cl_2 is placed in a modified NMR tube, the solvent is evaporated, and Rh(OEP)(PEt_3) (400 μL of 10 mM solution in C_6D_6) is added; the tube is shaken several times; the color changes rapidly to red; the ^1H NMR and UV−visible spectra are those of Rh(OEP)(PEt_3)PF_6 (vide infra). MS (+ESI) $C_{42}H_{59}N_4PRh$ calcd 753.35, found 753.39 (cluster).

Rh(TPP)$(PEt_3)_2$. To a solution of HRh(TPP) (2.5 mg, 3.5 μmol in 400 μL of C_6D_6) is added 25 μL of a 0.72 M solution of PEt_3 (18 μmol, 5 equiv) in C_6D_6; the color changes from brown-red to bright green; only free PEt_3 resonances are observable in an ^1H NMR spectrum; UV−visible spectra show absorption bands attributable only to the oxidized species, $Rh(TPP)(PEt_3)_2^+$ presumably by oxidation with adventitious O_2. A sealed NMR sample changes color to greenish-brown within 2 h with concomitant appearance of the resonance corresponding to $Rh(TPP)(PEt_3)_2^+$ and partial precipitation; no resonances attributable to the anion are detected in ^1H NMR spectrum. MS (+ESI) $C_{56}H_{58}N_4P_2$-Rh calcd 951.32, found 951.15. Reactions with O_2 in an EPR tube and $FeCp_2PF_6$ were done exactly as described above.

Rh(por)(PEt_3)PF_6. In a drybox, Rh(por)I (2.5 mL of a toluene solution, 1 mg/mL) is mixed with PEt_3 (50 μL of 70 mM solution in toluene); the solvent is removed after 5 min yielding IRh(por)(PEt_3): (por = OEP) ^1H NMR ($CDCl_3$) δ 10.12 (s, 4H, meso), 4.14 (m, 7 Hz, 8H, CH_2), 3.96 (m, 7 Hz, 8H, CH_2), 1.91 (t, 7.5 Hz, 24H, CH_3), −1.73 (dt, 8 Hz, 15 Hz, 9H, phosphine CH_3), −3.40 (dq, 8 Hz, 1.5 Hz, 6H, phosphine CH_2); UV−vis (3M PEt_3 in toluene, λ_{max}/nm) 367, 436, 538. por = TPP ^1H NMR ($CDCl_3$) δ 8.79 (s, 8H, β-pyrolic), 8.24 (d, 8 Hz, 4H, o-Ph), 8.09 (d, 8 Hz, 4H, o′-Ph), 7.72 (m, 14H, m-, m′-, p-Ph), −1.42 (dt, 6 Hz, 7.5 Hz, 9H, phosphine-CH_3), −2.91 (dq, 3 Hz, 7.5 Hz, 6H, phosphine-CH_2); UV−vis (3M PEt_3 in toluene, λ_{max}/nm) 354, 398, 458, 520, 564, 604). IRh(por)(PEt_3) is dissolved in benzene/CH_2Cl_2 (2:1, 2 mL) and 150 μL of a 20 mM solution of $AgPF_6$ in toluene is added. The precipitate is collected and recrystallized from CH_2Cl_2/benzene/pentane (1:1:5) to give Rh(por)(PEt_3)PF_6 in 85−90% yield. The advantage of the stepwise procedure is that monoligated species can be prepared free of either the bisphosphine or the nonligated complexes. In our hands, one of these impurities was inevitably present in Rh(por)(PEt_3)(PF_6) samples obtained from addition of PEt_3 to Rh(por)I/$AgPF_6$ mixtures, as a result of an error in adding exactly 1 equiv of the phosphine: Por = OEP ^1H NMR ($CDCl_3$) δ 10.34 (s, 4H, meso), 4.11 (m, 7 Hz, 16H, CH_2), 1.90 (t, 7 Hz, 24H, CH_3), −1.72 (dt, 4 Hz, 7.5 Hz, 9H, phosphine-CH_3), −3.13 (dq, 4 Hz, 7.5 Hz, 6H, phosphine-CH_2); ^1H NMR (C_6D_6) δ 10.23, 3.99 (m, 7.5 Hz), 3.89 (m, 7.5 Hz), −1.97 (dt, 6.5 Hz, 7.5 Hz), −3.35 (dq, 3 Hz, 7.5 Hz). The higher degree of magnetic anisotropy on the two faces of the porphyrin plane in C_6D_6, as evidenced by the larger separation of the resonances of the diastereotopic methylene protons, is likely due to the formation of close ion pair between PF_6^- and $Rh(OEP)^+$ in the nonpolar solvent. UV−visible (toluene, λ_{max}/nm) 408, 517, 558 (depending on an excess of the free ligand, Rh^{III}(por)(PEt_3)PF_6 is present in equilibrium with $Rh(por)^+$ and $Rh(por)(PEt_3)_2^+$; the spectra for Rh(por)(PEt_3)PF_6 reported herein were obtain by deconvolution of the resulting UV−vis data). por = TPP ^1H NMR ($CDCl_3$) δ 8.66 (s, 8H, β-pyrolic), 7.91 (d, 7 Hz,

4H, o-Ph), 7.82 (d, 7 Hz, 4H, o′-Ph), 7.69 (t, 7.5 Hz, 4 H), 7.64 (t, 7.5 Hz, 4 H), 7.59 (t, 7 Hz, 4 H), −1.66 (dt, 17.5 Hz, 9 H, phosphine-CH_3), −3.02 (dq, 2.5 Hz, 8.5 Hz, 6H, phosphine-CH_2); UV−vis (toluene, λ_{max}/nm) 424, 540.

Rh(por)(PEt$_3$)$_2$PF$_6$ are prepared by simple addition of ≥1 equiv of PEt_3 in toluene to a toluene/CH_2Cl_2 (1:2) solution of the monoligated complex, removal the solvents in vacuo, and recrystallization of the residues by pentane layering of CH_2Cl_2/toluene (1:1) solutions: por = OEP ^{1}H NMR (C_6D_6) δ 10.20 (s, 4H, meso), 4.12 (q, 8 Hz, 16 H, CH_2), 1.89 (t, 8 Hz, 24 H, CH_3), −1.82 (quintet, 9.5 Hz, 18 H, phosphine-CH_3), −3.47 (q, 8 Hz, 12 H, phosphine-CH_2); UV−vis (3 M PEt_3/toluene, λ_{max}/nm) 362, 437, 537, 567. por = TPP ^{1}H NMR (C_6D_6) δ 8.84 (s, 8H, β-pyrolic), 8.19 (d, 6.5 Hz, 8 H, o-Ph), 7.50 (quintet, 14.5 Hz, 14 H, m-, p-Ph), −1.61 (quintet, 6.5 Hz, 18 H, phosphine-CH_3), −2.87 (br q, 7.5 Hz, 12 H, phosphine-CH_2); UV−vis (3 M PEt_3/toluene, λ_{max}/nm) 345 (sh), 364, 448, 558, 598.

Spectrophotometric Titrations. UV−visible samples were prepared in a drybox by addition of 25 μL of 1 mM stock solution of [Rh(OEP)PF_6]$_x$ (x = 1, 2) in CH_2Cl_2 to 2.5 mL of anhydrous toluene in a 10-mm quartz UV−visible cell, which was subsequently sealed with a septum. The solutions of the ligands of different concentrations were prepared in a drybox, placed in septum-sealed vials; each vial was placed in a septum-sealed Schlenk flask under N_2. Titrations were done by addition of an aliquot of the ligand (5−50 μL of 0.7 mM to neat phosphine or of 1 mM to neat pyridine) by a gastight syringe to the UV−visible cell, mixing the solution, measuring spectra every 2 min until the steady-state spectrum was achieved (6−8 min), and repeating the procedure. Resulting data were processed using the SpecFit 3.0.8 software package (Spectrum Software Associates) for global analysis of complex equilibrium data. The component spectra, identified by the software, agreed adequately with the spectra collected independently ($Rh(OEP)^+$, $Rh(OEP)py^+$, $Rh(OEP)(PEt_3)_2^+$). A total of three sets of data for each ligand were used: starting solutions for two sets were obtained by dissolving Rh(por)PF_6 and, for the third, by dissolving Rh(OEP)$(PEt_3)_2PF_6$ (or Rh(OEP)py_2PF_6), and the results were averaged. The bispyridine adduct, $Rh(OEP)py_2^+$, could not be obtained at the highest concentration of pyridine still miscible with toluene (Figure 6) and the upper limit of the corresponding K_2^{py} value was estimated by assuming that, at the final titration point, no more than 10% (the detection limit) of the total concentration was due to $Rh^{III}(OEP)py_2^+$: UV−vis (toluene, λ_{max}/nm) $Rh(OEP)^+$ 393, 513, 544, 552(sh); $Rh(OEP)py^+$ 407, 522, 554; isosbestic points (±3 nm) 401, 508, 536, 552. The 552-nm shoulder in the UV−visible spectrum of Rh(OEP)(PF_6) may be due to the presence of a minor impurity such as Rh(OEP)$(H_2O)(PF_6)$ (UV−vis (toluene, λ_{max}/nm) 403, 522, 553). However, since the titration data could be adequately described by a three-component model in the case of PEt_3 ($Rh(OEP)^+$, $Rh(OEP)(PEt_3)^+$, and $Rh(OEP)(PEt_3)_2^+$) and a two-component model in the case pyridine ($Rh(OEP)^+$ and $Rh(OEP)py^+$), the contribution of the possible aqua complex was not significant within the limits of the used mathematical procedures.

Acknowledgment. We thank NSF (Grant CHE-9612725) and Stanford Graduate Fellowship (R.B.) for financial support. The Mass Spectrometry Facility at University of California, San Francisco is supported by NIH (Grants RR 04112 and RR 01614).

JA001364U